ISABE-2015-20018

AERO ENGINE INTERCOOLING OPTIMIZATION USING A VARIABLE FLOW PATH

Xin Zhao
Ph.D. student
Chalmers University of Technology
SE-412 96 Göteborg, Sweden
xin.zhao@chalmers.se

Tomas Grönstedt
Professor
Chalmers University of Technology
SE-412 96 Göteborg, Sweden
tomas.gronstedt@chalmers.se

Abstract

A previous study showed a great reduction in SFC for an intercooled geared engine by controlling the coolant air of the intercooler at different flight conditions. This action reduces the intercooler external cold side irreversibility. However, the loss incurred in the intercooler internal hot side remains at a considerably high level at cruise. This paper introduces a variable flow path concept, where half of the intercooler internal hot flow bypasses the intercooler at cruise. A further reduction of 0.5% cruise SFC can be achieved for the intercooled geared engine with this control, resulting in a total of 4.9% fuel burn reduction compared with an optimized advanced geared engine.

Nomenclature

a	Major axis length of the elliptical tube
b	Minor axis length of the elliptical tube
D	Diameter
D_h	Hydraulic diameter of any internal passage
f	Friction factor
h	Heat transfer coefficient
j	Colburn j factor
K	Loss coefficient for ducts
k_{loss}	Tube internal loss coefficient
$\dot{m}$	Mass flow rate
p	Static pressure
P	Total pressure
T	Temperature
ρ	Density
ε	Roughness of the tube wall
μ	Dynamic viscosity
η	Polytropic efficiency
k	Thermal conductivity of air
Re	Reynolds number
Pr	Prantdl number
Nu	Nusselt number
St	Stanton number
BPR	Bypass ratio
FPR	Fan pressure ratio
HPC	High pressure compressor
IPC	Intermediate pressure Compressor
LPT	Low pressure turbine
OPR	Overall pressure ratio
PR	Pressure ratio
SFC	Specific fuel consumption
SFN	Specific thrust
TIT	Turbine inlet temperature
TOC	Top of climb
NEWAC	New Aero Engine Core Concepts
LEMCOTEC	Low Emissions Core-Engine Technologies

Introduction

In the foreseeable future, it is expected that air traffic will continue to grow at a steady pace. Accompanying the growth is an overloaded environment. More efficient and cleaner turbofans are

required to release the pressure brought about by the commercial aircraft emissions, i.e. carbon dioxide emissions and NO_x. An intercooled cycle, as can be found in basic thermodynamics books, is one possible solution that could give lower fuel consumption and lower emissions. By intercooling the air during the compression process, a lower combustor entry temperature can be obtained resulting in lower NO_x emissions at a given overall pressure ratio (OPR) and a given turbine inlet temperature (TIT). Furthermore, intercooling can improve engine efficiency by enabling a very high OPR, which is currently constrained by the turbine blade cooling.

In contrast to the intercooled stationary gas turbine, intercooler system design for aero engine applications is very challenging because of the limited space. In the EU 6th framework programme New Aero Engine Core Concepts (NEWAC), an intercooled core was proposed by Rolls-Royce UK for a long range large turbofan [1-3] with a 'V' shaped corrugated configuration. In order to maximize the benefit of the intercooled core, great efforts were devoted to minimize the installation penalty of the intercooler system [4, 5] and to reduce the pressure loss in the intercooler and its ducting system [6, 7].

An alternative intercooler configuration, a two-pass cross flow tubular intercooler, was first studied in NEWAC [8, 9] by Chalmers University of Technology and then developed further in the EU 7th framework programme Low Emission Core-Engine Technologies (LEMCOTEC) [10]. This tubular intercooler, as reported in [11-14], has shown a sufficient heat transfer capability with reasonable loss and size to be beneficial for the high OPR geared intercooled aero engines studied.

In addition, intercooled core concepts with a separate variable geometry exhaust nozzle were reported in [12, 14, 15], as illustrated in *Figure 1*. The separate nozzle, which is used to limit the coolant flow through the intercooler, can greatly reduce the pressure loss incurred by the intercooler external side and showed considerable improvement in cruise SFC. This intercooling control is simply based on the fact that, for aero engine applications, operating points such as take-off, top-of-climb and cruise result in different working conditions, and hence also in a varying demand for intercooling. Critical points, such as take-off and top of climb, require relatively large amounts of intercooling to allow for a high OPR compact engine design. On the other hand, while the ambient air temperature is dramatically reduced at cruise, intercooling can be turned down. With less intercooling, both the heat rejection from the core and the losses through the intercooler can be reduced.

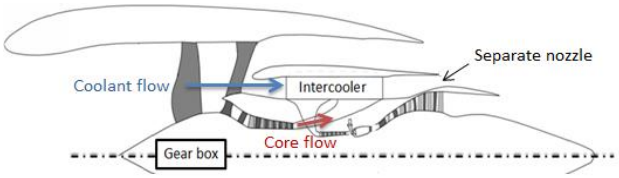

Figure 1 Illustration of an intercooled engine with a separate nozzle downstream of the intercooler

However, the separate nozzle functions for the intercooler external side only. For a geared intercooled core engine, similar conclusions have been drawn from sensitivity analyses made by different authors [13, 16]. The losses in the intercooler internal hot side are relatively more important than those in the external cold side. The exchange rates for a 1% pressure loss increase in the internal side and external side are around a 0.3% and

0.2% increase, respectively, in the block fuel. For the intercooled core studied here, a pressure loss of about 4% in the internal side is expected at cruise, which indicates a 0.6% block fuel reduction when half of the loss can be eliminated.

This paper presents a Variable Flow Path (VFP) concept controlling the hot side flow at different flight phases to further optimize aero engine intercooling control for a lower SFC. The effects of this concept on other relative properties, i.e. emissions and compressor performance, are also discussed.

Intercooler modeling with variable flow path

Original intercooler concept

The two-pass cross flow tubular intercooler developed in [10] is adopted to establish the intercooled geared turbofan optimization with a separate nozzle and VFP. This is identical to the previous studies [12, 14], where 24 intercooler modules are distributed annularly around the core. The original layout of a single module can be viewed in Figure 2. Flow exiting an intermediate compressor or high speed booster enters the inflow duct through which it is diffused. The flow then enters the first stack of a tubular heat exchanger located downstream in the cooling flow direction, returns to an upstream tubular heat exchanger and then continues to an accelerating duct leading to the high pressure compressor entrance. Bypass air flows over the external surfaces of the two tubular stacks to achieve the sought intercooling. The tubes are extended in an involute spiral way to give a good utilization of the space available, as shown in Figure 3. The general staggered tube configuration, which is the cross-section of the tube stack, can be seen in Figure 4, and the general parameters for the intercooler used in this paper are defined in Table 1.

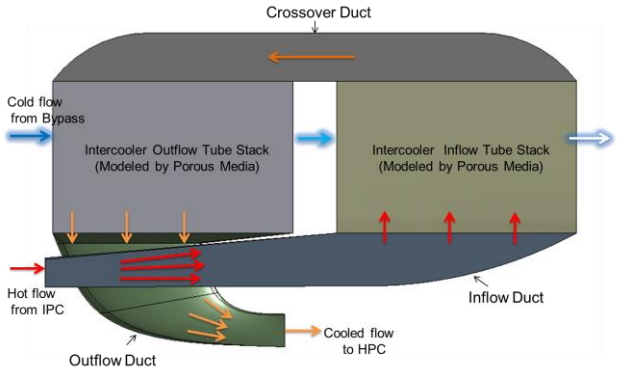

Figure 2 Two-pass cross flow tubular intercooler

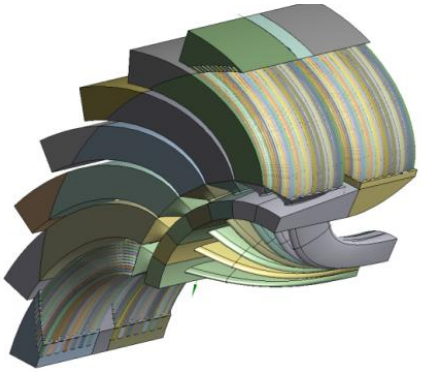

Figure 3 Involute spiral tube configuration installation

The CFD based correlations for the intercooler can be found in [10] and are given below:

Inflow duct (Reynolds number is based on the inflow duct inlet condition. Correlation is valid in the range of 500,000 to 1,400,000.):

$$K_{inflow\_duct} = -1.626 \times 10^{9} Re^{-1.837} + 0.5513 = \frac{p_{out} - p_{in}}{p_{0,in} - p_{in}} \quad 9)$$

Tubes (Pressure loss correlation from [17]. Heat transfer correlation from [18]):

$$\frac{1}{\sqrt{k_{tube}}} = -1.8\log_{10}\left(\frac{6.9}{Re} + \left(\frac{rough}{D}/3.7\right)^{1.11}\right) \quad 10)$$

$$Nu = \frac{(k_{tube}/8.0)(\mathrm{Re}-1000)\,\mathrm{Pr}}{1+12.7\sqrt{(\frac{k_{tube}}{8.0})}(\mathrm{Pr}^{2/3}-1)} \quad 11)$$

Crossover duct (Reynolds number is based on the crossover duct inlet condition. Correlation is valid in the range of 100,000 to 350,000.):

$$\mathrm{K}_{\mathrm{crossover_{duct}}} = 3.128\times10^{-7}\mathrm{Re} + 10.1 = \frac{\mathrm{p_{in}}-\mathrm{p_{out}}}{\mathrm{p_{0,in}}-\mathrm{p_{in}}} \quad 12)$$

Outflow duct (Reynolds number is based on the outflow duct outlet condition. The correlation is valid in the range of 1,500,000 to 5,500,000.):

$$\mathrm{K}_{\mathrm{outflow\_duct}} = 1.939\times10^{11}\mathrm{Re}^{-2.1} + 0.08107 = \frac{\mathrm{p_{0,out}}-\mathrm{p_{0,in}}}{\mathrm{p_{0,out}}-\mathrm{p_{out}}} \quad 13)$$

In the correlations above, p is the static pressure and $\mathrm{p_0}$ is the total pressure, while 'in' and 'out' subscripts represent the inlet and outlet of the duct, respectively; $rough$ is the roughness of the tube wall (a value of 0.002 mm is assumed here). The hydraulic diameter of the ducts and the tube are used to calculate the Reynolds number in the corresponding correlations.

External cold side – tube stacks
The Colburn j factor is used here. This is the dimensionless heat transfer coefficient as defined in [19]:

$$\mathrm{j} = \mathrm{St}\cdot\mathrm{Pr}^{2/3} = \frac{\mathrm{Nu}}{\mathrm{Re}\cdot\mathrm{Pr}}\mathrm{Pr}^{2/3} \quad 14)$$

The Nusselt number, the Reynolds number and the related hydraulic diameter used in the external cold side correlations are calculated as:

$$\mathrm{D_h} = \frac{4\mathrm{A_c}\mathrm{L}}{\mathrm{A_w}} \quad 15)$$

$$\mathrm{Nu} = \frac{\mathrm{h'D_h}}{\mathrm{k}} \quad 16)$$

$$\mathrm{Re} = \frac{(\dot{\mathrm{m}}/\mathrm{A_c})\mathrm{D_h}}{\mu} \quad 17)$$

where $\mathrm{h'}$is the local heat transfer coefficient, $\mathrm{D_h}$ is the hydraulic diameter of the intercooler tube stack flow passage, k is the thermal conductivity of air, $\mathrm{A_w}$ is the surface area of the ellipses, $\mathrm{A_c}$ is the minimum flow cross sectional area, L is the total flow length of the intercooler, $\dot{\mathrm{m}}$ is the mass flow at the inlet and μ is the dynamic viscosity.

The friction factor, f, is defined through [19]:

$$\Delta\mathrm{p} = \frac{(\dot{\mathrm{m}}/\mathrm{A_c})^2}{2\rho_{\mathrm{in}}}[\mathrm{f}\frac{\mathrm{A_W}}{\mathrm{A_c}}\frac{\rho_{\mathrm{in}}}{\rho_{\mathrm{m}}} + (1+\sigma^2)(\frac{\rho_{\mathrm{in}}}{\rho_{\mathrm{out}}} - 1)] \quad 18)$$

where $\Delta\mathrm{p}$ is the pressure drop through the intercooler, ρ_{in} and ρ_{out} are the fluid inlet and outlet densities, ρ_{m} is the average of ρ_{in} and ρ_{out}, and σ is the ratio between the minimum flow cross sectional area, $\mathrm{A_c}$, and the intercooler frontal area, $\mathrm{A_f}$. The correlations provided below are valid in the range of 10,000 < Re < 110,000. The largest deviation from CFD data is 0.90%.

$$\mathrm{j} = 0.003469\mathrm{e}^{-7.117\times10^{-5}\mathrm{Re}} + 0.003461\mathrm{e}^{-3.793\times10^{-6}\mathrm{Re}} \quad 19)$$

$$\mathrm{f} = 0.01044\mathrm{e}^{-6.806\times10^{-5}\mathrm{Re}} + 0.008109\mathrm{e}^{-2.908\times10^{-6}\mathrm{Re}} \quad 20)$$

The additional weight and nacelle diameter caused by the intercooler have also been considered. Titanium is assumed to be used as intercooler material based on its lightweight performance. The tube thickness is calculated on the basis of the pressure difference between the inner and outer side of the tube. A minimum tube thickness

is assumed to be 0.2 mm. The nacelle line moves with the change in intercooler size in order to keep the external bypass flow Mach number lower than 0.6.

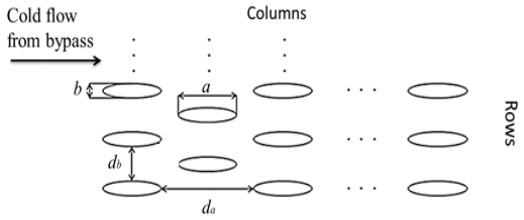

Figure 4 Intercooler external side heat transfer tube arrangement demonstration

a/b	8.0
d_a	a
d_b	$2b$
a (mm)	30.7
Tube length (m)	0.374
Number of tube rows	12
Number of tube columns	20
Intercooler weight (kg)	310

Table 1 Intercooler parameters for one tube stack

Variable flow path concept

Based on the intercooler concept described above, an offtake illustrated in *Figure 5* is added to

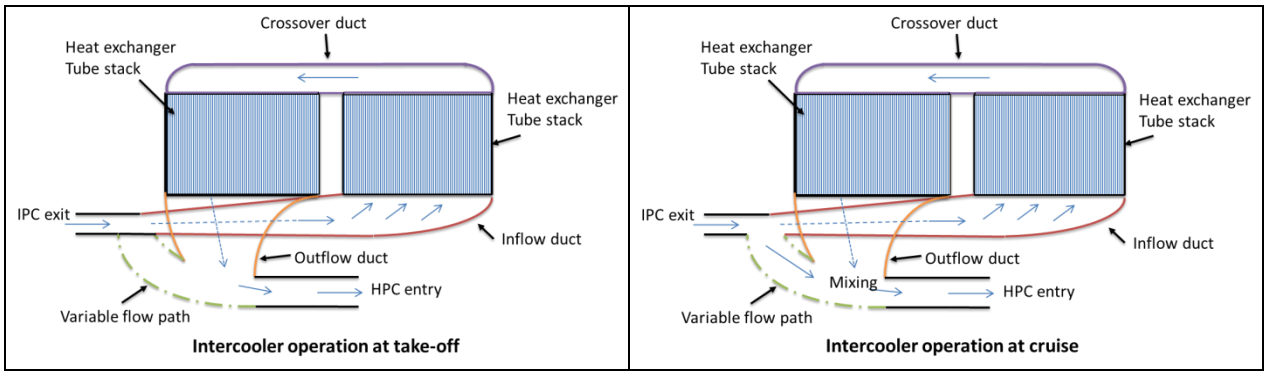

Figure 5 Two-pass cross flow intercooler with VFP

connect the inflow duct and outflow duct, directly forming a VFP duct for the intercooler. This duct, which can be switched on/off by a moving cylindrical shell, as shown in *Figure 6*, is determined to bypass part of the core flow during control. Keeping part of the high temperature core flow through the intercooler at cruise can effectively avoid icing problems for the thin and dense tubes. In addition, the space that remains after the intercooler installation is limited, and designing the path for part of the core flow will be more applicable.

To be able to maximize the benefit of this VFP concept, the flow split ratio between the VFP and the intercooler original path at cruise must be optimized. Additional relevant properties will be discussed later.

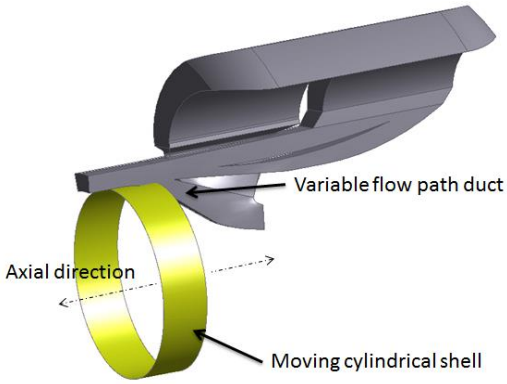

Figure 6 Moving cylindrical shell on-off for the VFP

Engine Modeling

The engine design point performance parameters common to all the engines studied in this paper is presented in Table 2. These are based on estimates of performance levels achievable for an engine entering into service in the year 2025. The efficiencies in the table are polytropic efficiencies. T_{blade} is the maximum permitted blade temperature. A hot day take-off condition is used to evaluate the engine at the start of the mission analysis. The cooling flow is then calculated on the basis of the model established in [20].

Parameter	Value
$T_{HPC,exit}$	< 950 K
$T_{Combustor,exit}$	< 1900 K
T_{blade}	< 1210 K
η_{fan}	93.5%
η_{IPC}	92.2%
η_{HPC}	92.5%
η_{HPT}	90.7%
η_{IPT}	91.4%
η_{LPT}	93.25%
Net Thrust	65625 lbf

Table 2 Design point performance parameters (take-off)

The optimization procedure establishes an engine that provides minimum fuel burn for a fixed mission and fixed aircraft. The mission length is 6800 km. The initial cruise altitude is 35000 ft and the final cruise altitude is 39000 ft. The engine take-off net thrust is set to 65625 lbf, which is considered suitable for the twin engine aircraft model used for this study. The basic aircraft conceptual design methodology is based on the methods presented in [21].

Non-intercooled geared reference engine

The optimized advanced non-intercooled geared engine established in previous work [12, 14] is adopted here as the reference engine. The key parameters of this engine can be found in Table 3. The OPR is limited by the turbine blade and disc cooling temperature, as manifested by a maximum compressor exit temperature of 950 K. The optimization of this engine was done by varying the bypass ratio (BPR), the fan, the intermediate pressure compressor (IPC) and the high pressure compressor (HPC) pressure ratios.

Intercooled geared engines

An intercooled reference engine with a separate variable geometry nozzle controlling the coolant mass flow was also established in this work. Details on key parameters of this engine are also given in Table 3. The OPR for the intercooled geared core is limited because the HPC exit blade height value has reached the point where the HPC efficiency starts to decrease at an unfavorable rate. A rule of thumb is that the compressor blade height should not be lower than 12 mm to avoid a rapid drop in HPC efficiency [11]. In addition to the variation of the BPR, FPR, IPC and HPC pressure ratios, this intercooled engine was also optimized by varying the openness of the separate nozzle, where 30% openness was found to be optimal.

The intercooled engine with both a separate nozzle and VFP is established by keeping the key parameters the same as in the reference intercooled geared engine with a separate nozzle. A simplified assessment was made to calculate the weight increase introduced by the VFP. With the use of titanium and a thickness of 2.0 mm, the total increase in

weight including the duct and moving cylindrical shell is about 25 kg, which is less than 1/10 of the intercooler installation.

	Ref. Non-IC geared	Ref. IC geared	VFP. IC geared
OPR	55	79	79
BPR	14.8	17.1	17.2
Fan PR (outer)	1.450	1.444	1.442
IPC PR	5.42	4.98	4.98
HPC PR	7.73	12.58	12.53

Table 3 Key parameters for the engines presented, take-off point

The duct loss of the VFP is estimated on the basis of the work in [22]. For a compressor duct design with $\frac{\Delta R}{L} = 0.5, \frac{h_{in}}{L} = 0.3$ and inlet/outlet area ratio of one, the net duct loss, Y_p, as defined below, is 0.04 [22].

$$Y_p = \frac{p_{0,in} - p_{0,out}}{p_{0,in} - p_{in}} \qquad (21)$$

In the description above, ΔR is the change in mean radius between the inlet and outlet of the duct, L is the duct axial length, h_{in} is the inlet height, p is the static pressure and p_0 is the total pressure, while 'in' and 'out' subscripts represent the inlet and outlet of the duct, respectively. Momentum balance and the mass weighted average enthalpy method are applied to model the mixing of the two flow streams, see [23]. The mixing loss is assumed to be of the same magnitude as the loss in the duct.

The optimization of the intercooled engine with both a separate nozzle and the VFP concept is to vary the mass flow through the VFP duct to find the minimum cruise SFC.

Results and discussion

Engine performance

The results from varying the mass flow through the VFP at cruise are shown in Figure 7. The curve indicates that the core flow split ratio close to 1 gives the lowest SFC. As the flow through the VFP increases, the engine benefits the most from the loss reduction through intercooler in the beginning, as shown in Figure 8.

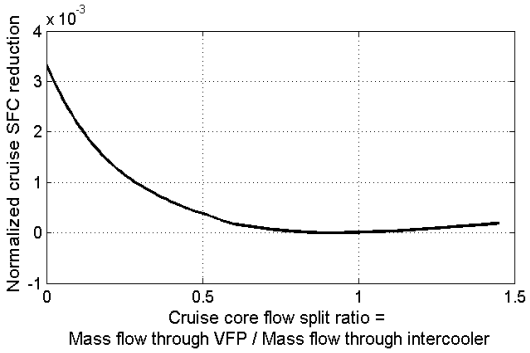

Figure 7 Normalized cruise SFC reduction for the intercooled engine with separate nozzle and VFP when mass flow is varied through the VFP at cruise

However, the decrease in SFC becomes slower because the loss through the intercooler is approaching the loss through the VFP duct; hence, no further significant improvement can be obtained. At the same time, the HPC entry temperature continues to rise at a steady pace, which increases the power requirement of the compressor and deteriorates the SFC benefit from reducing intercooling.

The key performance data in the three engines are given in *Table 4*. Unless specified as top-of-climb (TOC) or take-off (T/O) data, the values represent cruise (CR) performance because the VFP concept works only for the cruise point. Compared to the two reference engines, the VFP concept with half of the core flow passing through the VFP duct improves the cruise SFC by 3.7% and 0.5% respectively

as can be seen in Table 4. A trade factor was established to take into account that the reduced fuel burn can be used to reduce the aircraft operational empty weight and take-off weight. The trade factor also takes into account that the reduced take-off weight allows for a lesser aircraft drag and a reduced engine thrust. The value of the trade factor was estimated to be 1.5, which gives a net fuel burn reduction of 4.9% for the VFP concept compared with the non-intercooled engine.

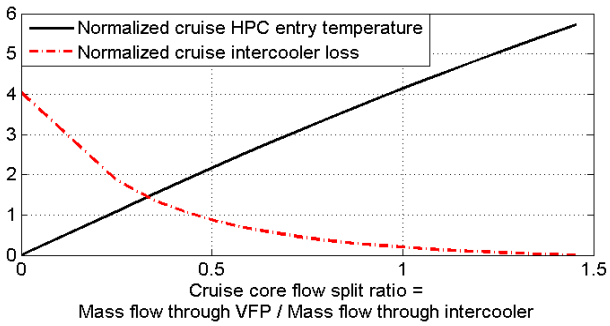

Figure 8 Normalized HPC entry temperature and intercooler loss for the intercooled engine with separate nozzle and VFP, varying mass flow through the VFP at cruise

Apart from the SFC and fuel burn, utilization of the VFP has several other effects on the engine components, particularly the HPC. First, the HPC compression becomes harder due to the increased HPC inlet temperature, and the pressure ratio then tends to move towards the IPC from the HPC. Meanwhile, the increased HPC inlet pressure due to the decreased intercooler internal pressure loss and increased low pressure compression system pressure ratios requires a lower HPC pressure ratio. In total, the power requirement of the compressors increases, but not too much. Consequently, the specific power of the core decreases and this must increase the total inlet mass flow.

Cruise Data	Ref. Non-IC geared	Ref. IC geared	VFP. IC geared
OPR	52	74.3	74.6
BPR	15.6	18.8	19.0
Fan PR (outer)	1.389	1.455	1.457
Fan mass flow (kg/s)	435.6	382.1	383.1
IPC PR	6.08	4.31	4.44
HPC PR	6.87	13.70	12.98
Core mass flow (kg/s)	26.73	19.73	19.66
VFP Mass flow (kg/s)	NA	NA	9.73
HPC exit temperature (K)	808	787	804
Turbine entry temperature (K)	1552	1701	1727
Jet velocity ratio	0.78	0.79	0.80
SFC (mg/Ns)	13.10	12.66	12.61
$\eta_{thermal}$	0.514	0.542	0.543
$\eta_{propulsive}$	0.822	0.807	0.808
Engine mass (kg)	6957	6700	6737
Nacelle diameter (m)	3.47	3.53	3.53
Mission fuel burn reduction (incl. trade factor)	Baseline	-4.5%	-4.9%
Engine architecture	1-7-7-1-4	1-5-9-1-5	1-5-9-1-5
HPC tip Mach number	1.33	1.37	1.31

Table 4 Engine cruise performance comparison between non-intercooled and intercooled geared configuration

The mixing of the two flow streams, one from the VFP duct and another from the intercooler outflow duct,

may affect HPC performance because of the temperature and pressure distortion. In fact, by pushing half of the core flow through the VFP duct, the pressure losses incurred in the two paths are quite similar, and a very light pressure distortion at the inlet of the HPC can be expected. On the other hand, the temperature distortion does exist and may result in a reduction of the surge margin [24]. However, investigation of this effect is not the purpose of this work.

In addition, there are two advantages of this concept beyond the facts discussed above. One is that the VFP duct can make the structure of the intercooler ducting system stiffer. Another is that the VFP can be used as a normal inter-compressor duct for passing all the core flow in the case of an emergency, i.e. intercooler failure.

Emissions estimation

As the carbon dioxide emissions are basically proportional to the fuel burn level, the amount of reduction in the carbon dioxide emissions will be the same as the fuel burn reduction, as shown in Table *4* and Table 5.

	CO_2 emission during cruise	NO_x emission		
		T/O	TOC	CR
Ref. non-IC	Baseline			
Ref. IC	-4.5%	-17%	-2.3%	-3.4%
VFP IC	-4.9%	-17%	-2.3%	+8.3%

Table 5 Emissions estimation for the reference engines and the intercooled engine with VFP

The NOx emissions were assessed by calculating the NOx severity parameter, S_{NOx}, as defined in [25, 26]:

$$S_{NOx} = \left(\frac{p3}{2964.5\text{kPa}}\right)^{0.4} * e^{\left(\frac{T_3 - 826.26\text{K}}{194.39\text{K}} + \frac{6.29 - 100\times war}{53.2}\right)} \quad (22)$$

where the 'war' stands for water-air-ratio. T_3 and p_3 are the pressure and temperature at the entry of the combustor. Here, in this assessment, the air is assumed to be dry. Due to the increase in the temperature and pressure at the entry of the combustor when the VFP kicks in at cruise, the severity of the NOx parameter increases. Considering the cruise SFC reduction, the NO_x emission during cruise can be corrected. It can be seen in *Table 5* that the intercooled engines could reduce NO_x emissions effectively even if the OPR is much higher than the non-intercooled engine. However, the introduction of the variable flow path concept deteriorates this effect.

As we all know, NO_x emissions are very sensitive to the combustor entry temperature, hence the HPC entry temperature in this study. It can be seen in Figure 7 that, after the split ratio 0.5, the improvement in SFC is quite modest. To balance the NO_x increase at cruise, setting the split ratio at 0.5 can avoid excessive NO_x increases due to the largely increased HPC entry temperature without sacrificing a large part of the SFC reduction for the VFP intercooled engine. The assessment gives a 3% NO_x increase instead of 8.3% when the VFP is set at 0.5 and the fuel burn reduction is reduced to 4.8% compared to the reference non-intercooled engine.

Conclusion

Via this performance optimization and comparative study, we can draw key conclusions about an intercooled engine using the concept of a variable flow path:

- A considerable reduction in SFC can be obtained through the loss reduction by bypassing flow through the variable flow path at cruise. With a trade factor of 1.5, a net fuel burn reduction of 4.9% is observed for the VFP intercooled geared engine compared to a non-intercooled geared engine.

- The bypassing of the core flow from the intercooler at cruise leads to an increase in the HPC inlet temperature resulting in a large increase in cruise NO_x. A trade-off thus needs to be made between cruise SFC and cruise NO_x.

- The utilization of the VFP leads to a decrease in the cruise HPC rotational speed.

Acknowledgments

This work is financially supported by the E.U. under the "LEMCOTEC – Low Emissions Core-Engine Technologies", a Collaborative Project co-funded by the European Commission within the Seventh Framework Programme (2007-2013) under the Grant Agreement n° 283216.

References

1. Wilfert, G., et al., New Environmentally Friendly Aero Engine Core Concepts. The 18th International Symposium on Air Breathing Engines, ISABE-2007-1120, 2007.
2. Rolt, A.M. and K. Kyprianidis. Assessment of New Aero Engine Core Concepts and Technologies in the EU Framework 6 NEWAC Programme. in ICAS 2010 Congress Proceedings, Paper No. 408. 2010.
3. Rolt, A. and N. Baker, Intercooled Turbofan Engine Design and Technology Research in the EU Framework 6 NEWAC Programme. Proceedings of the ISABE, 2009: p. 7-11.
4. Kwan, P.W., et al., Minimising Loss in a Heat Exchanger Installation for an Intercooled Turbofan Engine. Proceedings of the ASME Turbo Expo 2011, Vol 1, 2011: p. 189-200.
5. A'Barrow, C., et al. Aerodynamic Performance of a Coolant Flow Off-Take Downstream of an OGV. in ASME 2011 Turbo Expo: Turbine Technical Conference and Exposition. 2011. American Society of Mechanical Engineers.
6. Walker, A.D., J.F. Carrotte, and A.M. Rolt, Duct Aerodynamics for Intercooled Aero Gas Turbines: Constraints, Concepts and Design Methodology. Proceedings of ASME Turbo Expo 2009, Vol 7, Pts a and B, 2009: p. 749-758.
7. Walker, A.D., et al., Intercooled Aero-Gas-Turbine Duct Aerodynamics: Core Air Delivery Ducts. Journal of Propulsion and Power, 2012. 28(6): p. 1188-1200.
8. Xu, L. and T. Grönstedt, Design and Analysis of an Intercooled Turbofan Engine. Journal of Engineering for Gas Turbines and Power-Transactions of the ASME, 2010. 132(11).
9. Xu, L., Analysis and Evaluation of Innovative Aero Engine Core Concepts, in Applied Mechanics Department. 2011, Chalmers University of Technology: Gothernburg, Sweden.
10. Zhao, X. and T. Grönstedt, Conceptual design of a two-pass cross-flow aeroengine intercooler. Proceedings of the Institute of Mechanical Engineers, Part G: Journal of Aerospace Engineering, 2014.

11. Camilleri, W., et al., Concept description and assessment of the main features of a geared intercooled reversed flow core engine. Proceedings of the Institution of Mechanical Engineers, Part G: Journal of Aerospace Engineering, 2014.
12. Zhao, X., T. Grönstedt, and K.G. Kyprianidis, Assessment of the performance potential for a two-pass cross flow intercooler for aero engine applications, in Proceedings of the 20th international symposium on air-breathing engines. 2013: Busan, South Korea.
13. Camilleri, W., Anselmi, E., Sethi, V., Laskaridis, P., Rolt, A., and Cobas, P., Performance characteristics and optimisation of a geared intercooled reversed flow core engine. Journal of Aerospace Engineering, 2014.
14. Zhao, X., O. Thulin, and T. Grönstedt. First and second law analysis of an intercooled turbofan engine. in Proceedings of ASME Turbo Expo 2015: Turbine Technical Conference and Exposition. 2015. Montreal, Canada.
15. Kyprianidis, K.G., et al., Assessment of Future Aero-engine Designs With Intercooled and Intercooled Recuperated Cores. Journal of Engineering for Gas Turbines and Power-Transactions of the ASME, 2011. 133(1).
16. Kyprianidis, K.G. and A.M. Rolt, On the Optimization of a Geared Fan Intercooled Core Engine Design. Journal of Engineering for Gas Turbines and Power, 2015. 137(4): p. 041201.
17. Haaland, S.E., Simple and Explicit Formulas for the Friction Factor in Turbulent Pipe-Flow. Journal of Fluids Engineering-Transactions of the ASME, 1983. 105(1): p. 89-90.
18. Gnielinski, V., New Equations for Heat and Mass-Transfer in Turbulent Pipe and Channel Flow. International Chemical Engineering, 1976. 16(2): p. 359-368.
19. Kays, W.M. and A.L. London, Compact heat exchangers. 2. ed. McGraw-Hill series in mechanical engineering. 1964, New York: McGraw-Hill.
20. Wilcock, R.C., J.B. Young, and J.H. Horlock, The effect of turbine blade cooling on the cycle efficiency of gas turbine power cycles. Journal of Engineering for Gas Turbines and Power-Transactions of the ASME, 2005. 127(1): p. 109-120.
21. Avellan, R. and T. Grönstedt, Preliminary Design of Subsonic Transport Aircraft Engines. Paper No. ISABE, 2007. 1195.
22. Naylor, E.M., et al., Optimization of nonaxisymmetric endwalls in compressor s-shaped ducts. Journal of Turbomachinery, 2010. 132(1): p. 011011.
23. Grönstedt, T., Development of methods for analysis and optimization of complex jet engine systems. 2000, Chalmers University of Technology: Sweden.
24. Braithwaite, W.M., E.J. Graber Jr, and C.M. Mehalic, The effects of inlet temperature and pressure distortion on turbojet performance. 1973.
25. Vera-Morales, M. and C. Hall, Modeling performance and emissions from aircraft in the aviation integrated modelling project. Journal of Aircraft, 2010. 47(3): p. 812-819.
26. Gleason, C.C. and D.W. Bahr, Experimental Clean Combustor Program: Phase III Final Report. 1979, NASA.